Chapter 4

The DØ detector

R. Jesik, F. Stichelbaut, K. Yip, A. Zieminski

The DØ Run II detector [1] shown in Fig. 4.1 builds on the detector's previous strengths of excellent calorimetry and muon detection in an extended rapidity range. The major addition to the apparatus is a precision tracking system, consisting of a silicon vertex detector surrounded by an eight layer central fiber tracker. These detectors are located inside a 2 T solenoid magnet.

4.1 The silicon vertex detector

The silicon vertex detector(SMT), shown in Fig. 4.2, is a hybrid barrel and disk design. The central detector, covering $|z| < 32$ cm, consists of six barrels with disks interspersed between them. Each barrel module consists of four radial layers of detector ladders located at a radius of 2.7, 4.5, 6.6, and 9.5 cm, respectively. Layers one and three have 50 μm pitch double sided silicon microstrip detectors (with axial and 90° strips) in the four inner barrels, and have single sided (axial strip) detectors in the two end barrels. Layers two and four have double sided detectors with axial and 2° stereo strips. Each disk module has twelve wedge-shaped double sided detectors (extending radially from 2.7 to 10 cm) with 30° stereo angle. The forward detector consists of six disks of similar design (three located near each end of the central detector) plus four larger 24-wedge disks made of single sided detectors, located at z = ± 110 cm and ± 120 cm. The detector is read out using SVX-II chips and has 800,000 total channels. The silicon vertex detector provides tracking information out to $|\eta| = 3$ and gives a reconstructed vertex position resolution of 15-40 μm in $r - \phi$ and 75-100 μm in z, depending on the track multiplicity of the vertex.

4.2 The central fiber tracker

The central fiber tracker consists of 74,000 scintillating fibers mounted on eight concentric carbon fiber cylinders at radii from 19.5 to 51.5 cm. Each cylinder supports four layers of fibers, one doublet in the axial direction and one doublet oriented at a 3° helical stereo angle for odd numbered cylinders and at $-3°$ for even ones. The fibers are multi-clad and have a diameter of 830 μm. Clear fiber waveguides carry the light for about ten meters

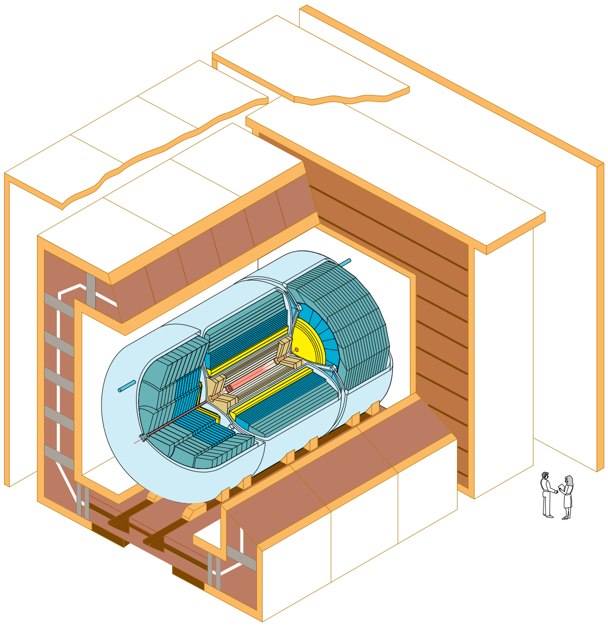

Figure 4.1: The DØ detector

from the scintillating fibers to the visible light photon counters situated in cryostats under the calorimeter. These are silicon devices that have a quantum efficiency of over 80% and a gain of about 50,000. They operate at a temperature of about 10 K. Digitization is also performed with SVX-II chips and the axial fibers are used to form fast level 1 trigger track objects.

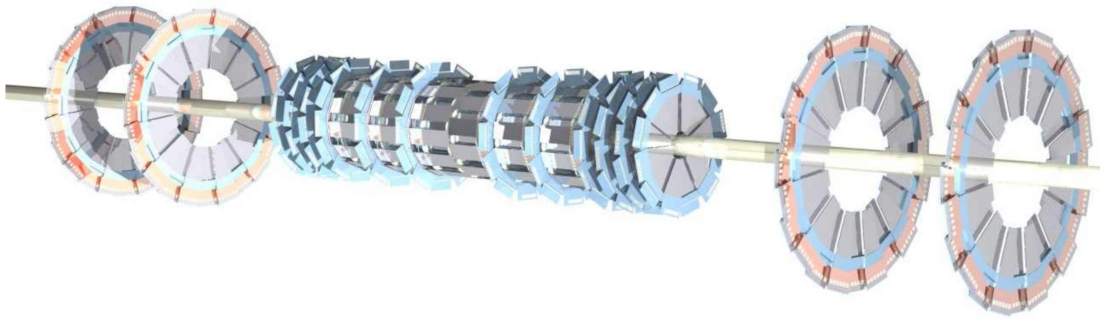

Figure 4.2: The DØ silicon vertex detector

The combined silicon vertex detector and central fiber tracker have excellent tracking performance. The full coverage of the entire combined detector extends out to $|\eta| = 1.6$. Tracks will be reconstructed with high efficiency ($\sim$ 95% in the central region) with a resolution of $\sigma_{p_T}/p_T^2 \sim 0.002$. The silicon detector disks allow efficient tracking out to an $|\eta|$ of 3.

4.3 Electromagnetic pre-shower detectors

Another important piece of the upgrade is the new pre-shower detectors attached to the inner surfaces of the calorimeter cryostats. These scintillating strip detectors greatly improve electron identification by providing a finer grain spatial match to the inner tracker than is obtained by the calorimeter alone. This reduces electron trigger backgrounds by a factor of 5-10. We will be able to trigger on electrons with p_T down to 1.5 GeV/c, and out to an $|\eta|$ of 2.5.

The calorimeter itself remains unchanged from its Run I configuration. It is a uranium-liquid argon sampling calorimeter with fine longitudinal and transverse segmentation, $\Delta\eta \times \Delta\phi = 0.1 \times 0.1$, that allows electromagnetic showers to be distinguished from hadronic jets. It has full coverage out to $|\eta| = 4$ with energy resolutions of $15\%/\sqrt{E}$ for electromagnetic showers and $80\%/\sqrt{E}$ for hadronic jets.

4.4 Muon Spectrometers

The central part of the muon system (covering the $|\eta| < 1$ range) includes 94 proportional drift tubes (PDT), barrel scintillator counters (A-PHI) and cosmic ray veto scintillator counters. There are three PDT layers (A, B, and C) with three or four 5-cm-thick, $\pm$5-cm-wide drift cells per layer. A $r - \phi$ magnetic field, with an average magnitude of 16.7 kGauss, is contained in an iron toroid sandwiched between layers A and B of the PDT system. The A-PHI counters have nine segments in the z direction and 80 segments in the ϕ direction. There are 630 A-PHI counters in total.

The forward muon system (located at both endcaps) covers the η $[\pm 1, \pm 2]$ region of the DØ detector. It includes mini-drift tubes (MDT's with A, B, and C layers) with three or four decks of 1-cm square cells per layer. Iron toroids are located between the A and B layers of the MDT systems. The average magnitude of the field is 16.0 kGauss. Three layers of PIXEL scintillating counters, located next to corresponding MDT stations, have a 4.5° ϕ-segmentation and a 0.1 η-segmentation.

The upgraded muon system offers excellent efficiency, purity, and coverage. We are able to trigger on muons with p_T down to 1.5 GeV/c, and out to an $|\eta|$ of 2.

4.5 Trigger system

Significant upgrades to the trigger and data acquisition systems are also required to operate in the high luminosity ($L = 2 \times 10^{32}\mathrm{cm}^{-2}\ \mathrm{S}^{-1}$), high rate (7 MHz) environment of the upgraded TeVatron. The DØ Run II trigger consists of three levels.

4.5.1 Trigger levels

The first level (L1) trigger consists of signals from the axial layers of the CFT, the preshower detectors, the calorimeter, and the muon scintillators and tracking chambers. The level 1 trigger hardware for each of these systems examine the event and report information to an array of front-end digitizing crates which have sufficient memory to retain data from 32 crossings. Trigger decisions are made in less than 4.2 μs at this level, providing deadtimeless operation with a maximum accept rate of 10 kHz. Upon a level 1 trigger accept, the entire event is digitized and moved into a series of 16 event buffers to await a level 2 decision.

The level 2 (L2) trigger will reduce the L1 accept rate of 10 kHz by roughly a factor of 10 within 100 μs by correlating multi-detector objects in an event. In the first stage, or preprocessor stage, each detector system builds a list of trigger information. This information is then transformed into physics objects such as energy clusters or tracks. The time required for the formation of these objects is about 50 μs. These objects are then sent to the level 2 global processor where they are combined and trigger decisions are made. For example, spacial coorelations between tracking segments, pre-shower depositions, and calorimeter energy depostions may all be used to select electron candidates. The deadtime of the level 2 trigger is expected to be less than 5%.

The third and final stage (L3) of the trigger will reconstruct events in a farm of PC processors with a final accept rate of 50 Hz.

4.5.2 Level 1 muon triggers

DØ Level 1 muon trigger (L1MU) [3] identifies muon candidates by using combinatorial logic that makes use of tracks from L1 Central Fiber Tracker (L1CFT) trigger and hits from all muon detector elements: drift chambers and scintillation counters. The central, north and south regions of the detector are divided into octants. The L1MU triggers are formed locally in each octant. For the purpose of this report the L1MU trigger terms are labelled by two digits and two letters : L1MU(i, j, A, B).

- The first number refers to the number of muons requested:
- The second number corresponds to an approximate value of the muon p_T threshold in GeV/c. The nominal values are 2,4,7 and 11 GeV/c.
- The first letter refers to the covered η^μ region:
  - C = Central, with $\mid \eta^\mu \mid \leq 1$;
  - A = All, with $\mid \eta^\mu \mid \leq 1.6$;
  - X = eXtended, with $\mid \eta^\mu \mid \leq 2$.
- Finally, the second letter describes the muon tag criterium:
  - M stands for Medium tag, requiring a L1CFT track matched with the PDT or MDT centroids, and with at least one layer-scintillator confirmation.

– T stands for Tight tag, requiring a L1CFT track combined with the PDT or MDT centroids, and with a two layer-scintillator confirmation.

4.5.3 Level 1 muon trigger rates and efficiencies

Performance of various muon triggers was evaluated in Ref. [2]. For this analysis we concentrated on:

- the single muon trigger L1MU(1,4,A,T)
- and the dimuon trigger L1MU(2,2,A,M).

The η^{μ} coverage of both triggers extends to $\mid \eta^{\mu} \mid \leq 1.6$ and effective muon p_T thresholds are 2 GeV/c for the dimuon trigger and 4 GeV/c for the single muon trigger. Muons with $p_T > 1.5$ GeV/c have a chance to penetrate the calorimeter, muons with $p_T > 3.5$ GeV/c have a chance to be detected in the entire muon detector, including B and C layers outside of the toroid magnet.

To estimate the QCD trigger rates, we used the dijet ISAJET events generated in 6 p_T intervals (2–5, 5–10, 10–20, 40–80 and 80–500) with 1, 3, 5 or 7 additional minimum bias interactions (p_T between 1 and 100 GeV/c) per event. The background trigger rates were computed with the assumptions of an instantaneous luminosity of 2×10^{32} cm^{-2}s^{-1}, a beam crossing time interval of 132 ns and a dijet total cross section of 57 mb. Studies of Ref. [2] indicate that the expected Level 1 trigger rates at this instantaneous luminosity are approximately 400 Hz and 80 Hz for the L1MU(2,2,A,T) and L1MU(1,4,A,T) triggers, respectively. The event samples used in these studies contained about 1000 events each. Therefore some rate calculation could suffer from large fluctuation due to the small number of selected events. The absolute rates obtained from these samples could be underestimated by a factor up to two.

For the trigger efficiency studies we have used a sample of $B_d^0 \rightarrow K_s + J/\psi$ events processed through the latest version of D0GEANT and the trigger simulator. Trigger efficiencies are normalized to the numbers of events with $\mid \eta^{\mu} \mid < 1.6$ and kinematic cuts imposed on p_T^{μ}, and $p_T^{\mu\mu}$ as specified in the Table 4.1. A large difference between efficiencies for the L1MU(1,4,A,M) and L1MU(1,4,A,T) triggers reflects the fact that the "tight" tag condition requires two scintillator signals for each muon. This requirement reduces the geometrical acceptance of the trigger due to a limited coverage of the scintillating counters at the bottom of the detector.

The trigger rates at the instantenous luminosity of 2 $10^{32} cm^{-2} s^{-1}$ due to dimuons from the genuine $Q\bar{Q}$ signal are $\approx$ 13 Hz ($\approx$ 4 Hz for $p_T^{\mu\mu} > 5$ GeV/c). The 13 Hz combines contributions from: $c\bar{c}$ pair production (2.5 Hz), $b\bar{b}$ pair production (9.5 Hz) and $b \rightarrow J/\psi + X$ decays (1.0 Hz). A requirement of dimuon $p_T^{\mu\mu} > 2$ GeV/c reduces the rate to 9 Hz.

To estimate the contribution from J/ψ production to the single muon trigger rate, we normalized the relevant Monte Carlo samples ($b \rightarrow J/\psi + X$ and prompt J/ψ's) to the

$p_T^{\mu\mu}$	> 2.0 GeV/c	> 5.0 GeV/c	> 5.0 GeV/c
p_T^{μ}	> 1.5 GeV/c	> 1.5 GeV/c	> 3.0 GeV/c
L1MU(2,2,A,M)	27%	46%	57%
L1MU(1,4,A,M)	33%	69%	78%
L1MU(1,4,A,T)	15%	32%	49%
dimuon or single (M)	41%	71%	80%
dimuon or single (T)	32%	55%	67%

Table 4.1: Trigger efficiencies for dimuon events preselected with the kinematic cuts listed

CDF measurement of the J/ψ cross sections in the kinematic range $p_T^{J/\psi} > 5$ GeV/c and $|\eta(J/\psi)| < 0.6$ [5]. With this normalization we find that the irreducible L1 trigger rate for signal events is at least 4.0 Hz for prompt J/ψ's and 0.8 Hz for J/ψ's from b-quark decays (J/ψ with $p_T^{J/\psi} > 2$ GeV/c and $|\eta^{J/\psi}| < 1.5$).

4.5.4 Level 2 and Level 3 muon triggers

The second level of the muon trigger (L2MU) uses calibration and more precision timing information to improve the quality of muon candidates. Fast processors and a highly parallelized data pathway are the basis of the L3 muon trigger (L3MU). L3MU improves the resolution and the rejection efficiency of L2MU candidates. This is accomplished by performing local muon tracking, by adding inputs form the calorimeter and the sillicon micro-strip tracker (SMT) and by performing more analytical calculations on CFT tracks and PDT and A-PHI hits with the calibrated data. The performance of the L2MU and L3MU triggers has not been fully evaluated at the time of this writing.

In addition, we expect to have the STT (Silicon Tracker Trigger) preprocessor installed in the middle of 2002. The STT will be part of the Level 2 trigger and will provide an option of triggering on displaced vertices (impact parameter significance). It will also further improve momentum resolution of muon tracks.

The STT will allow to tag B decays using displaced secondary vertices or tracks with large impact parameters. The expected impact parameter resolution in the transverse plane can be parametrized as [2]:

$$\sigma^2(d_0) = (12.6\ \mu\mathrm{m})^2 + \left(\frac{36.6\ \mu\mathrm{m}\, GeV}{p \times \sin^{3/2}\theta}\right)^2 \tag{4.1}$$

This dependence on particle momentum and polar angle is illustrated in Fig. 4.3.

In Fig. 4.4 we show the impact parameter significance, $S = d_0/\sigma(d_0)$, for the $B_d^0 \to K^{*\circ}\mu^+\mu^-$ decay products, under the condition that all four charged particles are produced with $p_T \geq 0.5$ GeV/c (muons with $p_T \geq 1.5$ GeV/c). On the average 1.8 particles from the $B_d^0 \to K^{*\circ}\mu^+\mu^-$ decay will have an impact parameter significance greater than 2.

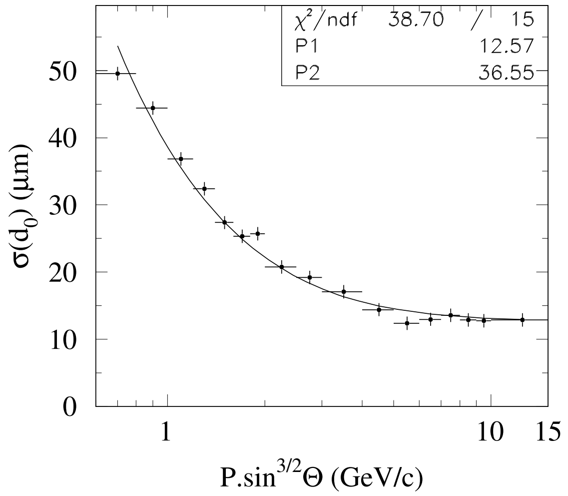

Figure 4.3: Expected impact parameter uncertainty dependence on track momentum and polar angle.

This number increases to 3.2 for events preselected by a request of a 400 μm transversal separation between primary and secondary vertices.

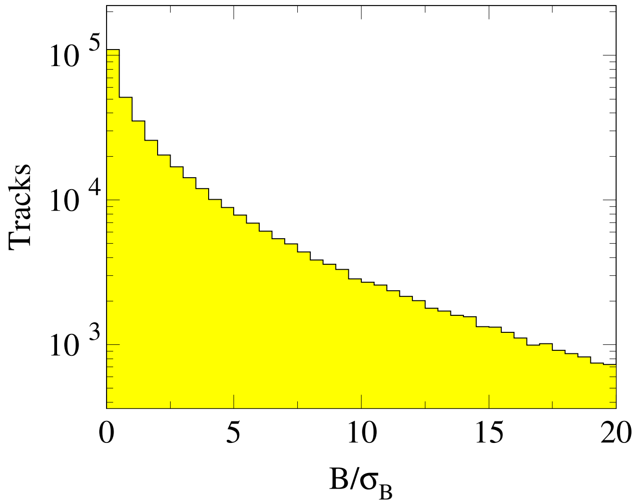

Figure 4.4: Significance distribution for STT tracks reconstructed in $B_d^0 \to K^{*\circ}\mu^+\mu^-$ events with all four charge particles produced with $p_T \geq 0.5$ GeV/c.

Therefore, once STT becomes operational, we intend to use a simple B tagging algorithm based on the number of tracks in the event with a significance greater than S_{min} to improve our Level 2 trigger rates for selecting $b\bar{b}$ events. The algorithm was tested on charged tracks with $p_T > 0.5$ GeV/c; $\mid \eta \mid < 1.6$; and with hits in at least 3 layers of the SVX [2]. As shown in Fig. 4.5 an efficiency of 50% can be achieved by requesting at least two tracks per event with an impact parameter significance greater than 2. Similarily, requiring at least one track with an impact parameter significance greater than 5 permits the reduction of

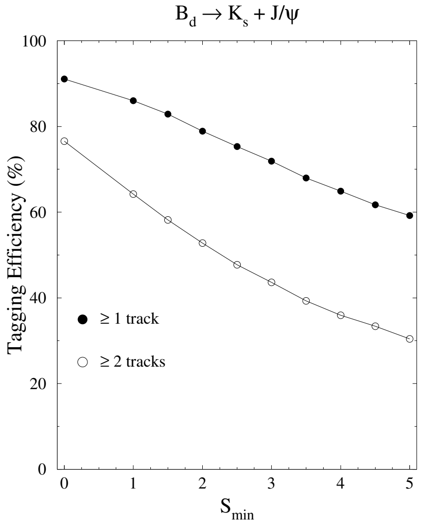

Figure 4.5: $b\bar{b}$ event tagging efficiency as a function of S_{min} with either one or two tracks in the event satisfying the condition $S > S_{min}$.

the background rate by a factor 10 while keeping 50% of the signal (assuming a primary vertex smearing of 30 μm).

Finally, we have studied the effect of the STT trigger on the separation of the J/ψ signal due to b-quark decays from the prompt J/ψ production. In case we need to suppress the prompt J/ψ signal, requiring at least one track with $\mid S_B \mid > 2.5$ provides a factor 7 reduction at the 30% cost to the non-prompt J/ψ signal.

4.5.5 Low p_T dielectron trigger

DØ has also introduced a dielectron trigger [4] aimed at detection of soft electron pairs, primarily from J/ψ dielectron decays. Level 1 electron candidates are selected with a transverse energy deposit $E_T > 2.0\ GeV$ in the EM calorimeter trigger towers, and with a low $\mathrm{p_T} > 1.5$ GeV/c track coincident with a pre-shower cluster. The two "electrons" are required to have opposite signs and to match within a quadrant in ϕ with the EM deposits. In the forward rapidity region ($1.5 < |\eta| < 2.5$) the trigger is based on EM deposits and preshower clusters only, since no tracking coverage is available.

The dielectron Level 2 trigger is based on a refined spatial matching between tracks and 0.2×0.2 EM trigger towers as well as on the information on the EM fraction of the clusters and their isolation. Finally, invariant mass and angular criteria are applied to select J/ψ dielectron decays.

Efficiencies and rates for this trigger have been estimated using *ISAJET* generated events overlaid with 2 extra interactions. Trigger rates at the nominal Run II luminosity are expected to be below 1 kHz at Level 1 and about 150 Hz at Level 2. The expected yield of triggered $B_d^0 \to J/\psi\ K_s^0$ events is 15×10^3 for an integrated luminosity of $2\,\mathrm{fb}^{-1}$.

References

[1] S. Abachi *et al.* *"The DØ upgrade"*, DØNote 2542, `http://www-d0.fnal.gov/hardware/upgrade/upgrade.html`.

[2] F. Stichelbaut, M. Narain and A. Zieminski, *Triggers for B Physics Studies in Run II*, DØ note 3354 (December 1997).

[3] K. Jones *et al.*, `http://hound.physics.arizona.edu/l1mu/l1mu.htm`; C. Leonidopoulos (for the DØ Collab.) CHEP 2001 talk - in press.

[4] P. Grannis and A. Lucotte, *"Extending the sensitivity to sin(2β) in the* $B^0/\bar{B}^0$ *system using a low pt electron* $J/\psi \rightarrow e^+e^-$ *trigger at the upgrade DØ detector"*, DØ Note 3596 (1999).

[5] F. Abe *et al.*, CDF Collaboration, Phys. Rev. Lett. **76**, 4675 (1996).

[6] DØ RunII GEANT, `http://www-d0.fnal.gov/newd0/d0atwork/computing/MonteCarlo/`.